Quantum well states, resonances and stability of metallic overlayers

2008 J. Phys.: Condens. Matter 20 315002

(http://iopscience.iop.org/0953-8984/20/31/315002)

J. Phys.: Condens. Matter **20** (2008) 315002 (8pp) doi:10.1088/0953-8984/20/31/315002

Quantum well states, resonances and stability of metallic overlayers

E Ogando[1], N Zabala[2,3], E V Chulkov[3,4] and M J Puska[5]

[1] SGIker, Ikerketa Errektoreordetza, UPV/EHU, Sarriena sn, 48940, Leioa, Spain
[2] Elektrizitatea eta Elektronika Saila, Zientzia eta Teknologia Fakultatea UPV/EHU 644 PK, 48080 Bilbao, Spain
[3] Donostia International Physics Center (DIPC) and Unidad Física de Materiales, CSIC-UPV/EHU, Apartado 1072, 20080 Donostia, Spain
[4] Materialen Fisika Saila, Kimika Fakultatea, UPV-EHU 1072 PK, 20080 Donostia, Spain
[5] Department of Engineering Physics, Helsinki University of Technology, PO Box 1100, FIN-02015 HUT, Finland

E-mail: nerea.zabala@ehu.es

Received 23 March 2008, in final form 28 May 2008
Published 26 June 2008
Online at stacks.iop.org/JPhysCM/20/315002

Abstract
The role of quantum well states (QWSs) and quantum well resonances (QWRs) in the stability of metallic overlayers is studied. When the substrate presents a confining gap, as it is the case of Cu(111), the stability is determined by QWSs and there is experimental evidence of the existence of magic thicknesses. For overlayers which do not have QWSs, as those grown on Al(111), we explore the existence of thicknesses of enhanced stability due to QWRs by comparing the strength of the oscillations in the surface energy.

(Some figures in this article are in colour only in the electronic version)

1. Introduction

It is well known that confinement of valence electrons in low-dimensional systems has a strong influence on their physical and chemical properties [1–6], in particular, on their stability or size distribution, giving rise to most stable or magic sizes. Ultrathin metal films are an example, where the confinement perpendicular to the surfaces produces a one-dimensional quantum well and the ensuing quantum well states (QWSs). But in these systems electrons are free along the directions parallel to the surfaces forming two-dimensional subbands. Moreover, quantum size effects (QSEs) affect the layered structures and are able to produce self-assembled structures on surfaces. They play an important role in applications based e.g. on the giant magnetoresistance [7] effect or magnetic coupling in multilayer structures [2].

The importance of QWSs on the stability of metallic thin layers, i.e. the electronic growth mode, has been proved on the growth of metals on semiconductor or metallic substrates by using scanning tunneling microscopy (STM) [8], helium-atom scattering [9–11] or surface x-ray diffraction [11, 12]. For example, under proper conditions Pb islands of preferred heights with a double monolayer (ML) periodicity, called 'magic islands', grow on Cu(111) [8] or Si(111) surfaces [13]. In some cases the effect is quite dramatic, enabling the growth of unusually stable films of magic thicknesses and uniformity on atomic level. Besides the Pb overlayer, Ag deposited on Fe(100) shows the electronic growth mode with films of 1, 2 and 5 ML thickness proved especially stable [14].

In the above-mentioned overlayer systems the electron confinement is due to a reflecting barrier at the interface caused by the gap in the substrate band structure projected onto the plane parallel to the interface, and the vacuum barrier. In a previous publication [15] we demonstrated the importance of describing correctly the substrate energy gap, in order to explain quantitatively the existence of magic heights. In practice we introduced a one-dimensional pseudopotential model [16] which contained the key characteristics of the band structure for the direction perpendicular to the interface and allowed us to reproduce with great accuracy the occurrence of magic heights in Pb islands on Cu(111) measured in the experiments by Otero *et al* [8]. Strain relief or lattice mismatch effects can affect drastically the shape evolution of the islands in the early stages of island growth, but they are out of the scope of the present study [17, 18].

Even in the absence of a confining energy gap, quantum well behavior has been reported for metal films absorbed on

a substrate; an example is Na on Al(111) [19–21]. States extending over the whole system display resonant character, so they are called quantum well resonances (QWRs). These states have been measured in photoemission spectra. Indeed, due to the large effective potential step between overlayer and substrate (the average effective potential is lower in Al), the character of electrons when moving in the Na region clearly differs from that in the substrate. Very recently, Altman [22] has studied Ag films on W(110) using low energy electron microscopy. He reported that quantum well resonances above the vacuum level play an important role and that the resonances are very sensitive to the film thickness.

In this paper we perform self-consistent DFT (density functional theory) calculations using a one-dimensional effective potential for the whole overlayer–substrate system. First we go through the case of Pb/Cu(111), for which the quantitative comparison with the experimentally measured magic islands heights [15] was published elsewhere. For Pb/Cu(111) both QWSs and QWRs exist but the stability is determined by QWSs close to the Fermi level, at the energy range of the Cu(111) band gap [15]. Later on, in systems which do not present QWSs, such as Na/Al(111), we explore the possibility of stabilization determined by QWRs sinking below the Fermi level as the slab thickness increases. We study the importance of the presence of a gap in the electronic structure of the substrate by comparing the oscillations of the surface energy of different overlayers, with different substrate band structures. For comparison, we provide a general analytical description of the energy oscillations for all the overlayers studied. Finally we explore the role of the potential step at the overlayer/substrate interface.

2. Electronic structure

The present calculations are performed in the framework of DFT [23] within the local density approximation (LDA) [24, 25]. We consider infinitely-extended films with perfect translational invariance, i.e. a homogeneous free electron gas, along the surface (the xy plane). The method used for the modeling of the metallic overlayers was presented in [16] and illustrated for Pb layers grown on Cu(111). A one-dimensional pseudopotential is constructed for the whole system, which contains the essential features for the strength of the confining barriers at the overlayer, accounting correctly for the energy gap of the Cu(111) substrate and using a stabilized jellium model [26, 27] for the overlayer. For the Na/Al(100) system we follow the same method to construct the one-dimensional pseudopotential which varies along the z direction (perpendicular to the surfaces) and accounts properly for the width of the energy gap of the substrate and its position with respect to the Fermi level [28]. For the Al(111) substrate, due to its free electron character (its energy gap is negligible for our calculations), we have used simply the stabilized jellium model. The effective potentials used to model the Na overlayers on both substrates are shown in figure 1.

Then, the Kohn–Sham equations are solved numerically only in the z direction (a one-dimensional problem) using the effective one-dimensional potentials described above.

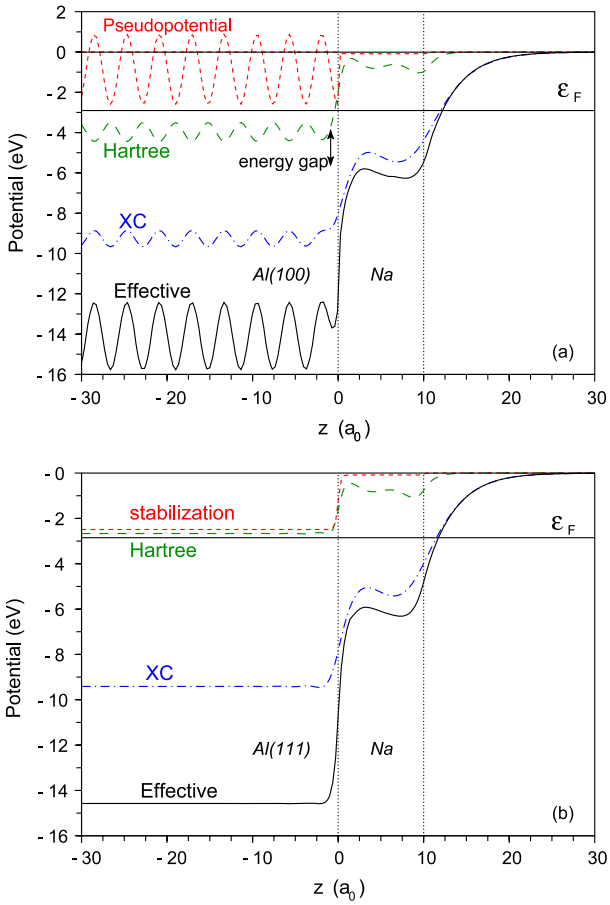

Figure 1. Effective potentials (continuous lines) used to model the Na/Al(100) (a) and Na/Al(111) (b) overlayers as a function of the distance to the Na/Al interface. The Hartree and exchange correlation (XC) contributions are shown as dashed and dashed–dotted lines, respectively. The short dashed line in (a) corresponds to the pseudopotential used for Al(100) and the stabilization term in Na. The later stabilizes the jellium at a given density against expansion or shrinkage. In (b) the short-dashed line corresponds to stabilization terms for Al and Na. For Na it is quite negligible. In (a) the vertical two-headed arrow corresponds to the Al(100) gap close to the Fermi level, given by the horizontal line.

The equations are discretized in a regular one-dimensional mesh and solved with the Rayleigh quotient multigrid method [29, 30], implemented in the real-space MIKA package [31] for electronic structure calculations. Hence, single-particle wavefunctions take the form

$$\Phi(\mathbf{r}) = \psi_n(z)\mathrm{e}^{\mathrm{i}\mathbf{k}_\parallel\cdot\mathbf{r}_\parallel}, \qquad (1)$$

where $\psi_n(z)$ is the wavefunction perpendicular to the surface, and plane waves are used parallel to the surface. In practice, our computational system is a finite slab of substrate material (comprising 25 Cu(111) layers) covered on both sides by the overlayer. The energy eigenvalue spectrum is then discrete but, as seen in figure 3 below, the resonance states can be recognized in the density of states because the resonance width is clearly larger than the separations between the energy eigenvalues. For further technical details, see Ogando *et al* [16].

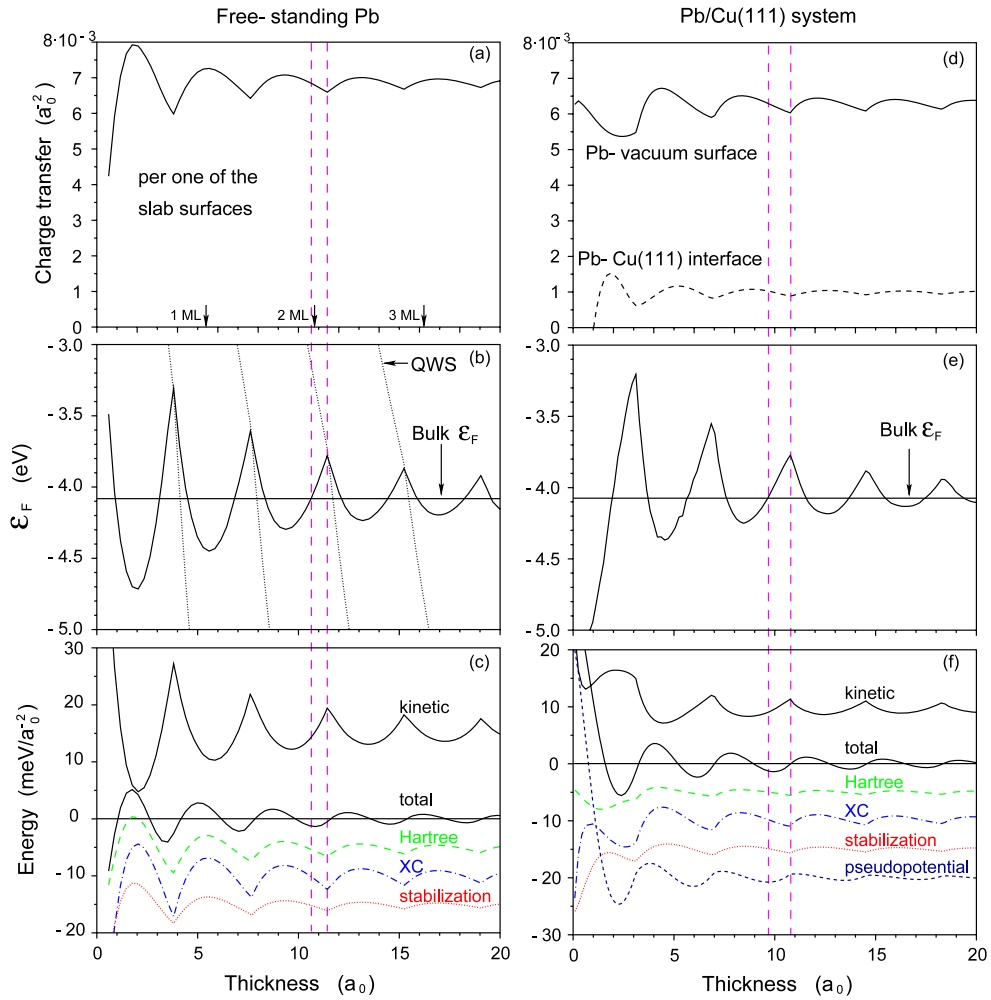

Figure 2. Comparing results for the free-standing Pb slab ((a), (b), (c)) and Pb overlayers on Cu(111) ((d),(e), (f)) as a function of the Pb layer thickness. ((a), (d)) Charge transfer out of the Pb layer, ((b), (e)) Fermi level (solid lines) and the evolution of the QWSs energies (dotted lines) and ((c), (f)) total energy oscillations and different contributions (kinetic, exchange–correlation, and stabilization term). The curves have been vertically shifted. Vertical dashed lines are to guide the eye.

Computationally, the stability of the overlayers can be understood in terms of the surface energy, which has local minima corresponding to the most stable thicknesses [15]. The total energy of the system can be separated in different contributions, $E_{\text{total}} = E_{\text{overlayer}} + E_{\text{substrate}} + E_{\text{interface}} + E_{\text{surface}}$, where $E_{\text{substrate}}$ and $E_{\text{overlayer}}$ are calculated by using the bulk energies corresponding to the substrate and overlayer metals, respectively. For the free-standing systems, $E_{\text{substrate}} = E_{\text{interface}} = 0$. The sum of the interface and surface energies, $E_{\text{interface}} + E_{\text{surface}}$, contains the oscillating part of the total energy.

3. Energy oscillations

To illustrate the origin of the energy oscillations, we first show in section 3.1 the contributions for free-standing Pb slabs and Pb overlayers supported on the Cu(111) substrate. In both cases energy oscillations are produced by QWSs. We have chosen the high electronic-density metal Pb because the oscillations in the contributions to the total energy are clearly visible. Then, in section 3.2 the electronic growth mode triggered by QWRs is analyzed by comparing systems with QWSs (Na overlayers on Cu(111)) and systems with QWRs (Na overlayers on Al(100) and Al(111)).

3.1. The role of QWSs: Pb/Cu(111)

We compare in figure 2 the results for free-standing Pb slabs (left) and Pb overlayer on Cu(111) (right) as a function of the slab or overlayer thickness. Figures 2(a) and (d) give the charge transfer out from Pb, i.e., the integrated electron density per unit area in vacuum and, for figure 2(d), also into the Cu substrate. Figures 2(b) and (e) show the behavior of the Fermi levels. The solid thick lines in figures 2(c) and (f) display the oscillations of the total energy and its different components. The oscillations are regular and their wavelength (3.77 a_0) is one half of the Fermi wavelength. For the free-standing Pb slabs figure 2(c) shows the contributions of both surfaces and for the Pb/Cu(111) system figure 2(f) includes the contributions of the Pb/vacuum surface and the Pb/Cu interface. The energy oscillations have been decomposed into the kinetic, Hartree, exchange–correlation

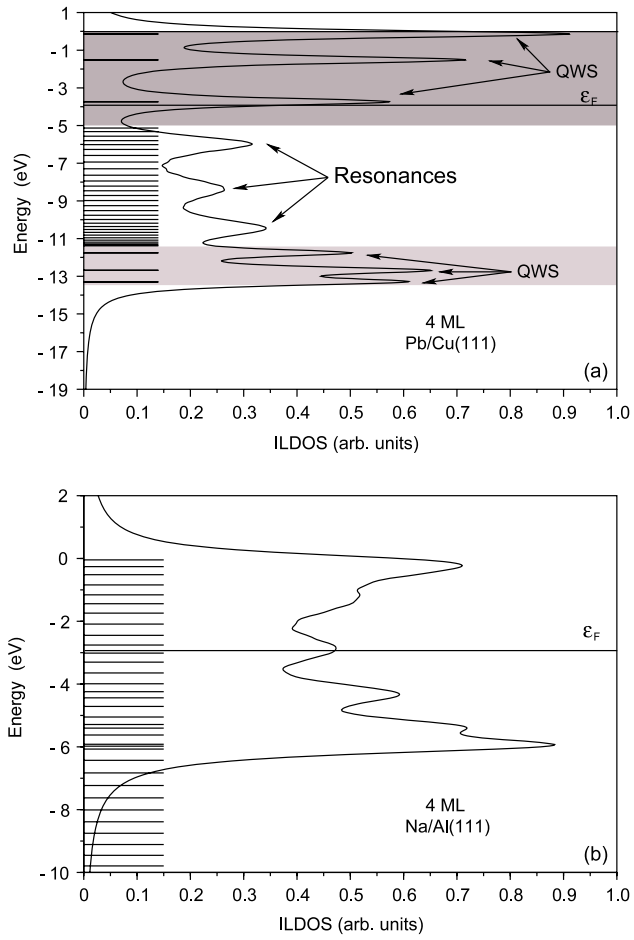

Figure 3. Integrated local density of states (ILDOS) for 4 ML Pb on Cu(111) and 4 ML Na on Al(111). The horizontal lines mark the energy eigenvalues. In (a) the gray areas denote the regions where QWSs appear. In (b) only resonances are present. Energies are given with respect to the vacuum level. The integration has been performed from the vacuum–overlayer surface to a depth of $11a_0$ inside the overlayer.

and stabilization (originating from the stabilized Pb potential) energies. For the Pb/Cu(111) system there is, in addition, the term corresponding to the Cu(111) pseudopotential.

We notice in figure 2 that the kinetic energy and the Fermi level show a peak when a QWS band starts to be populated. The oscillations in the kinetic energy happen because the lately occupied QWS band sinks, at first decreasing the kinetic energy. Subsequently the kinetic energy increases as a function of the film thickness due to the increased occupation of the parabolic subband until a new QWS band crosses the Fermi level.

The mechanism described above contributes only with a few meV to the Fermi level oscillations, which have an amplitude of about 1 eV. As stated by Schulte [32], the main component of the Fermi level oscillations arises because new QWSs below the Fermi level are weakly bound and their charge spills out of the film. The filling of these states increases the dipolar barrier pushing down the Fermi level. But when the last occupied QWS is strongly bound, the charge spilling and the surface dipole barrier reduce, raising the Fermi level, until the next QWS crosses the Fermi level. This is proved by comparing the Fermi level oscillations (figure 2(b)) and the charge per unit area transferred outside the edges of the jellium slab (figure 2(a)).

The different components of the energy in figures 2(c) and (f) reveal several trends. There is a direct correspondence between the charge transfer and the energy components corresponding to the potential terms: the larger is the charge transfer out of the slab or overlayer, where the potentials are lower, the larger are the potential energy components. In comparison with the free-standing Pb slab the Pb/Cu(111) system shows a strong reduction in the amplitude of the kinetic energy oscillations. This is related to the penetration of the wavefunction inside the Cu(111) substrate. The substrate also causes a new term arising from the electron–pseudopotential interaction.

We compare further results of the free-standing Pb slab and Pb/Cu(111) system. As expected, the charge transfers at the Pb–vacuum surface in figures 2(a) and (d) are similar, in absolute value and also in the amplitude of the oscillations (the small difference arises because, for computational reasons, the positive charge background surface-edge is smoothed, and the smoothing is slightly different in the two systems). The similar charge transfers toward vacuum lead to similar oscillations in the Fermi level in the two systems as well. The magnitude and oscillations of the charge transfer across the interface are much smaller than towards the vacuum. The smaller charge transfer oscillations together with the smaller average potential difference across the interface reduces remarkably the oscillations in the potential energy terms. In fact, comparing figures 2(c) and (f), the oscillations in the potential energy terms are mainly due to the Pb–vacuum surface contribution (the oscillations in the potential curves in figure 2(f) are approximately one half of the curves in figure 2(c), which contains the effects of two Pb–vacuum surfaces). Nevertheless the oscillations of the total energy are quite similar for the free-standing and supported systems, even though there is a reduction in the amplitude of its components.

Therefore, for both cases, Pb and Pb/Cu(111), it is not straightforward to deduce the shape of the energy curve from simple models. For example, the square infinite potential model includes only the kinetic energy term and it does not reflect the same oscillatory behavior of the total energy. Zhang *et al* [33] proposed a simple model that includes quantum confinement and charge spilling to calculate the energy of thin metallic films on semiconductor substrates. They calculated the kinetic energy term and the Fermi level with a square potential barrier of finite height at the surface and infinite height at the interface. The Hartree energy was evaluated using a classical capacitor to model the dipolar barrier at the interface, produced by the difference between the film and substrate Fermi levels and the ensuing charge transfer. This model reproduces qualitatively the results obtained self-consistently for Pb on a metallic substrate.

However, figure 2 shows that the Hartree contribution to the total energy at the film–substrate barrier is very small (it comes mainly from the Pb–vacuum surface). Our results point out that the Hartree term is only one of the components

and not the most important one. Besides, the bare infinite and/or finite potential barriers do not describe correctly the confinement of the wavefunctions either at the interface or at the surface. Therefore, although simple analytical models qualitatively describe the energy oscillations, their quantitative applicability [34, 33] should be carefully checked. We notice that our results describe unsupported slabs or slabs on metallic substrates. The appropriate description on semiconductors may be more difficult. Figure 2 shows that when a state crosses the Fermi level there is an inflexion in the energy curve.

3.2. The role of QWSs and QWRs: Pb/Cu(111), Na/Al(111) and Na/Al(100)

After the above analysis of QWSs we will focus on the behavior of QWRs, by studying the energy oscillations and their origin in different overlayers. But before, we compare the local density of states in Pb/Cu(111) and Na/Al(111) systems. Figure 3(a) shows the integrated local density of states (ILDOS) for 4 ML of Pb on Cu(111). The integration has been performed over the outermost 2 Pb ML with the total thickness of about 11 a_0. This thickness corresponds approximately to the electron emission depth in photoemission experiments. The LDOS itself is obtained by substituting the discrete eigenenergies by Lorentzian peaks with a width (FWHM) of 0.5 eV and weighting them by the local probability amplitudes of the states in question. The horizontal bars mark the eigenenergies, the gray areas show the regions where QWSs appear and the dark gray area corresponds to the energy gap of Cu(111) confining electrons in the overlayer. The light gray area, of minor importance because it is well below the Fermi level, is due to the different depths of the average Pb and Cu(111) potentials (the average potential is about 2 eV lower in Pb than in Cu(111)) [16, 15]. Notice that the ILDOS has sharp peaks corresponding to the QWSs. Furthermore, there are wider peaks in the continuous band region, which correspond to QWRs. Although there are no confined QWSs in this energy range, there are QWRs due to the potential step between Pb and Cu.

The QWRs have been recently measured for this system [35]. The clear character of the photoemission peaks leads the authors to state that 'these are not broadened enough to be classified as mere resonances'. Nevertheless, if one has a look at our figure 3 for 4 ML of Pb/Cu(111) we can distinguish the resonant origin of those peaks, because they are formed by several eigenstates. From the ILDOS (integrated over a layer of 11 a_0) calculated for the 20 ML Pb/Cu(111) system (as in the experiments) and plotted in figure 4, it is not straightforward to distinguish between QWR and QWS just by looking at the peaks.

If the Cu substrate is modeled just with the stabilized jellium model the Cu(111) energy band gap and ensuing QWSs disappear and QWRs emerge in the whole energy range. The total energy also shows oscillations in this case, but their amplitude is smaller than in our modeling [16, 15] in which QWSs are present. The amplitude of QWR oscillations at 5 ML of Pb on Cu(jellium) is similar to the amplitude at 20 ML of Pb on Cu(111). The jellium model is not adequate for the description of the QSEs in Cu substrates, but this comparison allows us to state that the resonances produced by a small Cu–Pb step (2 eV) are strong enough to produce magic islands of thicknesses of a few ML.

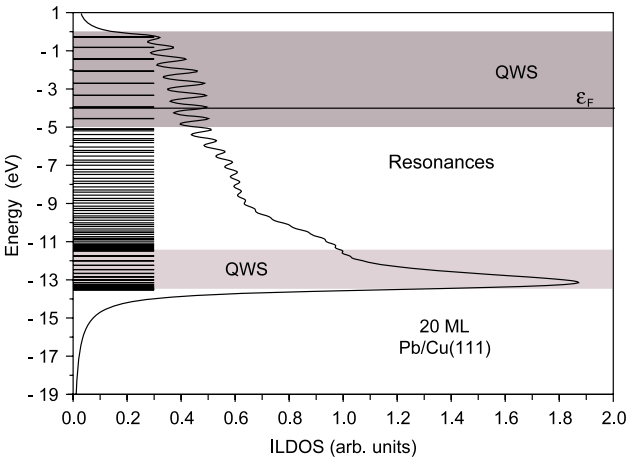

Figure 4. Integrated local density of states (ILDOS) for 20 ML Pb on Cu(111). The horizontal lines mark the energy eigenvalues and the integration has been performed from the vacuum–overlayer surface to a depth of $11a_0$ inside the overlayer.

Figure 3(b) shows ILDOS for 4 ML of Na on the Al(111) substrate described by stabilized jellium. This model can be used to describe the substrate in this case because, as we pointed out in the introduction, Al(111) has a gap but it is very narrow and well below the Fermi level. In this case the discrete energy levels have been substituted with Lorentzians of 0.6 eV width (FWHM). The jellium Al(111) substrate does not have an energy gap, so the peaks correspond only to resonant states.

In figure 5 the energy oscillations for Na on different substrates are shown as a function of the Na overlayer thickness. The points corresponding to integer numbers of Na ML have been marked by open circles (we chose the (111) direction but another direction does not alter the conclusions). For the Na/Cu(111) system the energy oscillations are mainly produced by QWSs crossing the Fermi level, while for Na/Al(100) and Na/Al(111) they are produced by QWRs. In the (100) direction aluminum has an energy gap from -1.15 to -2.83 eV with respect to the Fermi level, as it has been marked in figure 1. This energy gap, quite close to the Fermi level, increases the reflectivity of the Al substrate and the effect of resonances is stronger than in the case of Al(111) substrate. These differences in the substrate band structure explain the reduction of the oscillation amplitude from Na/Cu(111) through Na/Al(100) to Na/Al(111). Anyway, the amplitude of the oscillations for 5 ML coverage of the overlayer Na/Al(100), which has QWRs, is of the same magnitude as for the higher coverage of 8 ML in the overlayer Na/Cu(111), which has QWSs. The oscillations for Na/Al(111) are weaker and at 5 ML of Na they have the same strength as those for Na/Cu(111) at 11 ML of Na. To our knowledge, there are no works aimed at measuring magic islands or slab heights during the growth of Na. Nevertheless, by comparing the amplitudes of the energy oscillations in figure 6 and knowing that magic height islands have been found up to 35 ML of Pb on Cu(111),

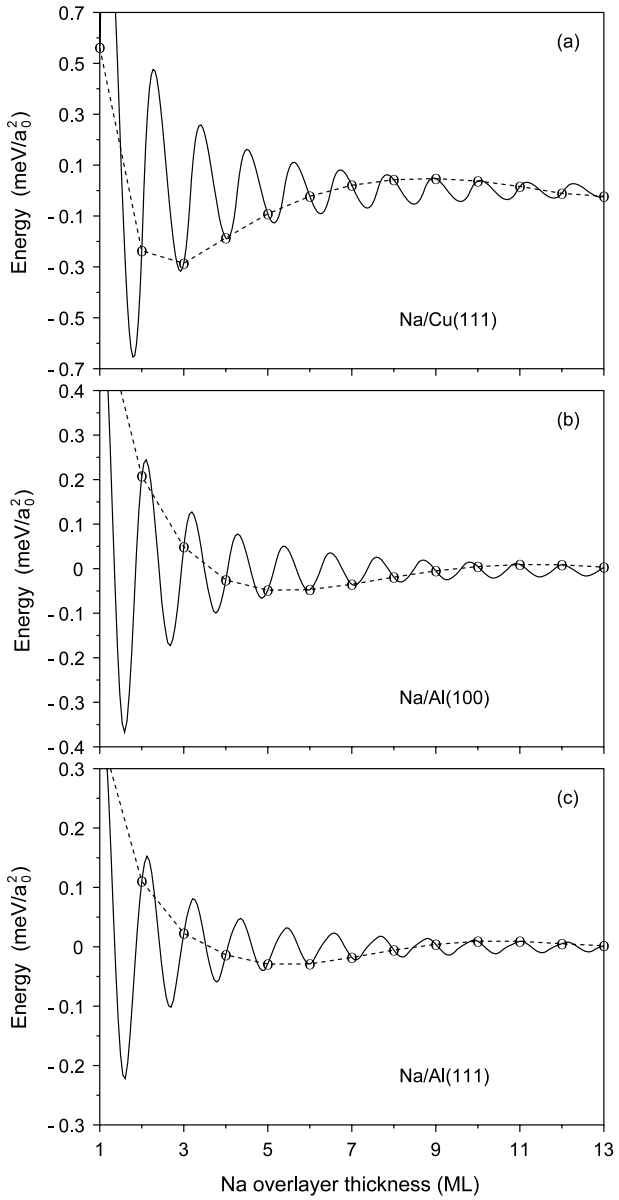

Figure 5. Oscillating part of the total energy per surface area for (a) Na/Cu(111), (b) Na/Al(100) and (c) Na/Al(111). The continuous lines are as a function of the continuous Na jellium thickness. The dashed lines connect the values corresponding to completed monolayers (ML) of thickness $d = 5.81a_0$.

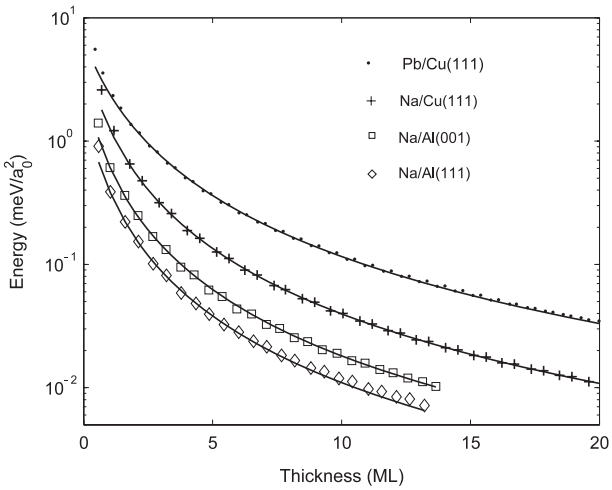

Figure 6. Damping of the amplitude of the energy oscillations for Pb/Cu(111), Na/Cu(111), Na/Al(100) and Na/Al(111). Each dot represents a maximum in the absolute value of the energy oscillation (e.g. see figure 5). The lines are fits using equation (3).

it should be possible that Na on Al forms islands or overlayers of enhanced stability due to QWRs.

The resonances are produced by the differences in the average potential depths between the substrate and the overlayer, but they are affected by the presence of an energy gap in the substrate. For Na/Al overlayers the potential is deeper in Al than in Na. Furthermore, for Na/Al(100) the resonances are enhanced with respect to Na/Al(111), due to the presence of an energy band gap close to the Fermi level in the Al(100) substrate. Other effects that may change the reflectivity at the interface, e.g. the lattice parameter mismatch, intermixing and disorder are not taken into account in our model. For instance, Stampfl *et al* [36] showed that Na can adsorb substitutionally into the first layer of Al(111) or Al(100). This would change the reflectivity at the Al/Na interface but, as we have pointed out, the contribution of this interface to the dependence of the energy on the thickness is expected to be less important than the contribution of the Al–vacuum surface.

4. Analytical description of the energy oscillations

As we have seen, the energy of the overlayers has a decreasing oscillatory behavior which can be described approximately with simple sine-like functions. Here we use a general formula to describe analytically the positions of the minima and the decreasing of the amplitude of the energy oscillations calculated self-consistently with the models described above for different overlayer–substrate systems, i.e.,

$$E_{\mathrm{osc}}(d) = F(d)\sin[2k_{\mathrm{F}}(d+\delta_0)]. \qquad (2)$$

Above, d is the film thickness and δ_0 is a phase, taking into account the confining properties of the substrate and surface and which can be experimentally determined; k_{F} is the Fermi wavevector of the overlayer. The function $F(d)$ is given later on. $d' = d + \delta_0$ is the effective width which confines the electrons at the Fermi level. With this formula we reproduce correctly the positions of the energy minima and maxima calculated self-consistently with our one-dimensional modeling of the overlayers.

The decay of the energy oscillations produced by the QSEs has been described with a $d^{-\alpha}$ law in different works, with α in the range of 1–2 [12, 37, 38]. For example, Czoschke *et al* [12] quote $\alpha = 0.938$ to fit the oscillations measured in Pb/Si(111) film nanostructures. To obtain the amplitude decay of the energy oscillations calculated with our model, we have taken their absolute values. The maxima obtained have been plotted in figure 6 for several systems, including Pb and Na overlayers on different substrates. A very good simple fitting

is obtained in all cases with an inverse square decay, i.e.,

$$F(d) = \frac{A}{(d+\delta_1)^2}, \tag{3}$$

where $(d + \delta_1)$ represents an effective width. The values obtained for δ_1 and δ_0 are not exactly the same, although they are of the same order in magnitude. On the other hand, we would like to notice also that this $\alpha = 2$ decreasing law has been found to govern the exchange coupling in magnetic multilayers [39, 40]. The different values of α obtained in other works are probably due to the omission of δ_1 in the function or considering the same value for δ_0 and δ_1.

Equation (2) provides an analytical description of the energy oscillations obtained from more sophisticated self-consistent calculations or measured experimentally, clearly improving previous formulas used in the literature [12, 37, 38]. We want to stress that this simple analytical expression is enough to describe the experiments or the results of more sophisticated calculations. However, in the model we have used, the parameters involved must be carefully chosen and checked when a quantitative agreement is required.

5. The potential step at the overlayer/substrate interface

As we have pointed out, the step of the potential at the interface overlayer–substrate is a key characteristic for the existence of resonances. To study the role of this step we have solved the analytical problem of the square potential shown in the insets of figure 7. A positive (negative) value of the Fermi energy difference between the overlayer and the substrate $\Delta = E_o - E_s$ means that the overlayer potential is deeper (shallower) than the substrate potential, corresponding to the sketch in figure 7(a) (figure 7(b)). Figure 7(b) could be a naive description of Na/Al overlayers.

The wavefunctions, ignoring the motion parallel to the surface, are $\psi_k(z) = A_k \sin(kz)$ in the overlayer and the non-decaying waves are given by $\psi_\chi(z) = B_\chi \sin(\chi z + \phi)$ in the substrate, where ϕ is a phase. The corresponding energies are $E_o = \hbar^2 k^2/2m_e$ and $E_s = \hbar^2\chi^2/2m_e$. By using the matching conditions and by integrating the wavefunction over the overlayer we obtain for the ILDOS

$$\mathrm{ILDOS}(E_o) = \frac{|B_\chi|^2}{\sin^2(kd) + \frac{E_o}{E_s}\cos^2(kd)}\left(\frac{d}{2} - \frac{\sin(2kd)}{4k}\right), \tag{4}$$

where d is the overlayer thickness. The fraction term in the front of the right-hand side is the amplitude $|A_k|^2$ and the term in parenthesis, of less importance, results from the integration over the overlayer. Figure 7 shows the ILDOS as a function E_o for different potential steps Δ. For $\Delta > 0$ the ILDOS is cut at the transition to the QWSs energy region, where the ILDOS is given as a sum of delta functions. For $\Delta < 0$ $(E_o/E_s < 1)$ the resonance peaks occur approximately when $\sin(kd) = 0$, i.e., the wavefunction has a node at the interface. The minima occur when $\cos(kd) = 0$. For $\Delta > 0$ $(E_o/E_s > 1)$ the resonance peaks occur approximately at $\cos(kd) = 0$, so that the wavefunction has an antinode at the interface and local scattering at the interface has stronger effects on the wavefunction [4] (in analogy to classical physics example of putting a finger at the antinode of a vibrating string).

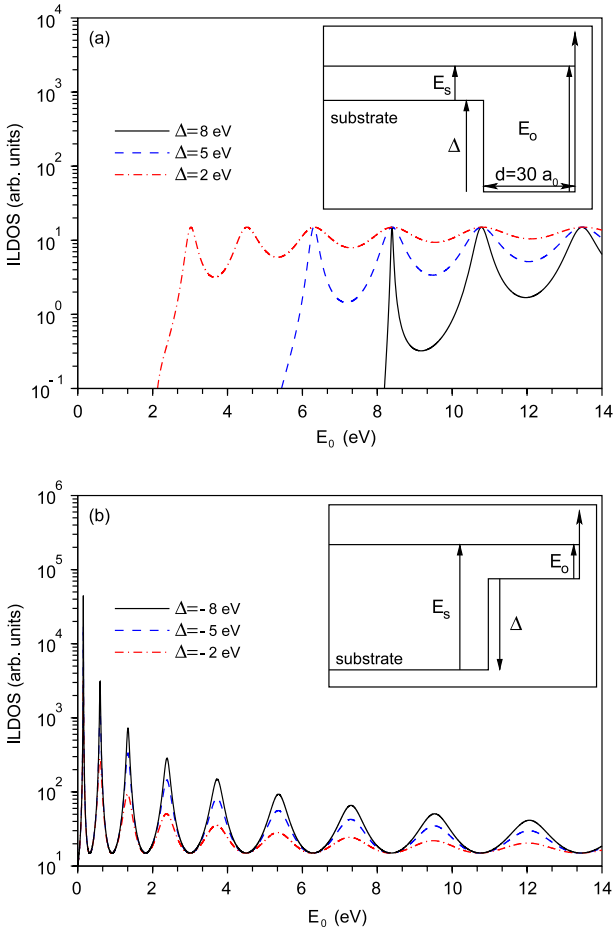

Figure 7. ILDOS (equation (4)) as a function of the energy E_o for the model systems shown in the insets and by using different values of the potential step Δ. The origin of energy is at the bottom of the overlayer potential.

The ratio between the ILDOS maxima and minima is E_s/E_o and the strength of the oscillations decreases strongly as a function of the energy (notice the vertical logarithmic scale). As expected, higher potential steps lead to stronger ILDOS oscillations. Therefore, systems with very different substrate and overlayer electron densities will show the clearest magic height selection due to resonances.

6. Conclusions

We have analyzed the stability and existence of magic heights of metallic overlayers by calculating the energy oscillations as a function of the number of monolayers. We have performed self-consistent calculations using a one-dimensional effective potential for the whole overlayer–substrate system, which gives a good description of the confinement barriers at the overlayer–vacuum surface and overlayer–substrate interface, including the effects of possible energy gaps of the substrate.

The results show that the main contribution to the oscillations arises from the vacuum–overlayer surface, whereas

the interface contribution is smaller. This difference is directly related to distinct strengths of the charge-spill-out oscillations. The boundary with the substrate has a smaller contribution to the energy oscillations, in comparison to that of the vacuum–overlayer surface.

We have provided a general analytical description for the decay of the oscillations with the overlayer coverage in all the systems studied, as an inverse square law.

The roles of QWSs and QWRs have been analyzed by comparing the ILDOS and energy oscillations in Pb/Cu(111), which has QWSs due to the existence of a confining gap at the Fermi level, and Na/Al(111) and Al(100), where there are only QWRs. We have proved that, in the latter case, the electronic growth mode of ultrathin films can be triggered by QWRs. The calculations also show that the presence of a substrate energy gap close to the Fermi level, as in the case of Na/Al(100), increases the reflectivity and the amplitude of the energy oscillations.

We want to notice some aspects that increase the strength of the effect of the QWRs. In the studied system (Na on Al) when selecting an integer number of monolayers the evolution of the energy curve is very smooth (figure 5) and this complicates the appearance of magic islands. Thin films of high electron-density metals show stronger variations in the energy as a function of the number of monolayers [15]. For example, the Na on Al system has approximately the same resonant character as Al on Na, but for the latter the energy changes from a minimum to a maximum, or vice versa, within just three monolayers. In this work we do not consider other interface scattering sources such as lattice parameter mismatch or disorder, which increase the reflectivity of the interface enhancing the QWRs.

On the other hand, a second quantum beating has been predicted for Pb thin films [41]. This re-entrance of QSEs recovers the amplitude of the energy oscillations and suggests that magic islands can be produced at higher thicknesses than currently measured. Thereby the argument that QWRs are able to determine magic islands is reinforced.

Acknowledgments

We acknowledge partial support by the University of the Basque Country and the Basque Hezkuntza Unibertsitate eta Ikerkuntza Saila (Grant No. IT-366-07), and Spanish MEC (FIS2007-65711-C02-01 and MAT2006-12743). The SGI/IZO-SGIker UPV/EHU (supported by the National Program for the Promotion of Human Resources within the National Plan of Scientific Research, Development and Innovation—Fondo Social Europeo, MCyT and Basque Government) is gratefully acknowledged for generous allocation of computational resources. This work was also partially supported by the Academy of Finland through its Centre of Excellence Program.

References

[1] Lindgren S Å and Walldén L 1987 *Phys. Rev. Lett.* **59** 3003
[2] Ortega J E and Himpsel F J 1992 *Phys. Rev. Lett.* **69** 844
[3] Paggel J J, Miller T and Chiang T C 1999 *Science* **283** 1709
[4] Kawakami R K, Rotenberg E, Choi H J, Escorcia-Aparicio E J, Bowen M O, Wolfe J H, Arenholz E, Zhang Z D, Smith N V and Qiu Z Q 1999 *Nature* **398** 132
[5] Chiang T C 2000 *Surf. Sci. Rep.* **39** 181
[6] Milun M, Peruan P and Woddneff D P 2001 *Rep. Prog. Phys.* **65** 99
[7] Ehrlich A C 1993 *Phys. Rev. Lett.* **71** 2300
[8] Otero R, Vázquez de Parga A L and Miranda R 2002 *Phys. Rev.* B **66** 115401
[9] Braun J and Toennies J P 1997 *Surf. Sci.* **384** L858
[10] Crottini A, Cvetko D, Floreano L, Gotter R, Morgante A and Tommasini F 1997 *Phys. Rev. Lett.* **79** 1527
[11] Floreano L, Cvetko D, Bruno F, Bavdek G, Cossaro A, Gotter R, Verdini A and Morgante A 2003 *Prog. Surf. Sci.* **72** 135
[12] Czoschke P, Hong H, Basile L and Chiang T C 2004 *Phys. Rev. Lett.* **93** 036103
[13] Altfeder I B, Matveev K A and Chen D M 1997 *Phys. Rev. Lett.* **78** 2815
[14] Luh D A, Miller T, Paggel J J, Chou M Y and Chiang T C 2001 *Science* **292** 1131
[15] Ogando E, Zabala N, Chulkov E V and Puska M J 2004 *Phys. Rev.* B **69** 153410
[16] Ogando E, Zabala N, Chulkov E V and Puska M J 2005 *Phys. Rev.* B **71** 205401
[17] Stepanyuk V S, Bazhanov D I, Baranov A N, Hergert W, Dederichs P H and Kirschner J 2000 *Phys. Rev.* B **62** 15398
[18] Prieto J E and Markov I 2007 *Phys. Rev. Lett.* **98** 176101
[19] Salmi L A and Persson M 1989 *Phys. Rev.* B **39** 6249
[20] Frank K H, Sagner H J and Heskett D 1989 *Phys. Rev.* B **40** 2767
[21] Barman S R, Haberle P, Horn K, Maytorena J A and Liebsch A 2001 *Phys. Rev. Lett.* **86** 5108
[22] Altman M S 2005 *J. Phys.: Condens. Matter* **17** 1305
[23] Jones R O and Gunnarsson O 1989 *Rev. Mod. Phys.* **61** 689
[24] Wang Y and Perdew J P 1991 *Phys. Rev.* B **43** 8911
[25] Ceperley D M and Alder B J 1980 *Phys. Rev. Lett.* **45** 566
[26] Perdew J P, Tran H Q and Smith E D 1990 *Phys. Rev.* B **42** 11627
[27] Shore H B and Rose J H 1991 *Phys. Rev. Lett.* **66** 2519
[28] Chulkov E V, Silkin V M and Echenique P M 1999 *Surf. Sci.* **437** 330
[29] Mandel J and McCormick S F 1989 *J. Comput. Phys.* **80** 442
[30] Heiskanen M, Torsti T, Puska M J and Nieminen R M 2001 *Phys. Rev.* B **63** 245106
[31] Torsti T, Heiskanen M, Puska M J and Nieminen R M 2003 *Int. J. Quantum Chem.* **91** 171
[32] Schulte F K 1976 *Surf. Sci.* **55** 427
[33] Zhang Z, Niu Q and Shih C K 1998 *Phys. Rev. Lett.* **80** 5381
[34] Yeh V, Berbil-Bautista L, Wang C Z, Ho K M and Tringides M C 2000 *Phys. Rev. Lett.* **85** 5158
[35] Dil J H, Kim J W, Gokhale S, Tallarida M and Horn K 2004 *Phys. Rev.* B **70** 045405
[36] Stampfl C, Neugebauer J and Scheffler M 2004 *Surf. Sci.* **307–309** 8
[37] Czoschke P, Hong H, Basile L and Chiang T C 2005 *Phys. Rev.* B **72** 075402
[38] Chiang T C 2004 *Science* **306** 1900
[39] Edwards D M, Mathon J, Muniz R B and Phan M S 1991 *Phys. Rev. Lett.* **67** 493
[40] Bruno P 1994 *J. Appl. Phys.* **76** 6972
[41] Ayuela A, Ogando E and Zabala N 2007 *Phys. Rev.* B **75** 153403